ARCHIVES OF METALLURGY
Volume 48 2003 Issue 4

MAREK FARYNA*/****, TOSHIMITSU OKANE**, EDWARD GUZIK***,
WALDEMAR WOŁCZYŃSKI****

ANALYSIS OF ORIENTED CRYSTAL GROWTH BY EDXS AND EBSD TECHNIQUES

ZASTOSOWANIE TECHNIK EDXS/EBSD W BADANIACH ZORIENTOWANEGO WZROSTU KRYSZTAŁÓW

A Fe-4.34Ni alloy was solidified directionally in the *Bridgman* system. The solid/liquid interface has been frozen and doublet structure revealed. Energy Dispersive Spectroscopy proved that peritectic reaction had occurred during solidification and modified profile of solute redistribution within primary phase existed just before peritectic reaction. Energ Dispersive X-Ray Spectrimetry (EDXS) solute measurements confirmed also the influence of doublet tip splitting on the solute redistribution. The obtained profile of solute redistribution modified by tip splitting has been compared to analogous profile obtained for the Al-3.5Li alloy in which doublet structure has also been formed but peritectic reaction does not exist. However, in the latter some precipitates have been predicted and revealed by use of the Scanning Electron Microscopy. Relevant equations have been formulated in order to fit experimental solute redistribution within frozen morphology of the Fe-4.34Ni alloy. The formulated equations are an analytical description of the peritectic reaction. It employs the *metastable solidus* line position known from the Fe-Ni phase diagram. An orientation of the doublet topography has also been determined based on electron backscatter diffraction (EBSD) acquired from the Al-3.5Li doublet shaped cells solidified and frozen during microgravity test.

Stop Fe-4.34Ni poddano krystalizacji w układzie *Bridgmana*. Zamrożono front krystalizacji dzięki czemu ujawniono istnienie struktury dubletonowej w stopie poddanym zorientowaniu. Pomiary techniką spektometrii energii dyspersji promieniowania rentgenowskiego (EDXS) wykazały zajście reakcji perytektycznej podczas krystalizacji. Przebieg reakcji zmodyfikował profil redystrybucji składnika, jaki istniał w fazie pierwotnej tuż przed zajściem reakcji perytektycznej. Zastosowanie tej samej techniki EDXS wykazało, że istnieje wpływ rozszczepienia

* ŚRODOWISKOWE LABORATORIUM ANALIZ FIZYKOCHEMICZNYCH I BADAŃ STRUKTURALNYCH, 30-060 KRAKÓW, UL. INGARDENA 3
** DIGITAL MANUFACTURING RESEARCH CENTER, THE NATIONAL INSTITUTE OF ADVANCED SCIENCE AND TECHNOLOGY, 1-2 NAMIKI, TSUKUBA, 305 8564 IBARAKI, JAPAN
*** INSTYTUT TECHNOLOGII I MECHANIZACJI ODLEWNICTWA, AKADEMIA GÓRNICZO-HUTNICZA, 30-059 KRAKÓW, UL. REYMONTA 23
**** INSTYTUT METALURGII I INŻYNIERII MATERIAŁOWEJ PAN IM. A. KRUPKOWSKIEGO, 30-059 KRAKÓW, UL. REYMONTA 25

wierzchołka dubletonu na kształt profilu redystrybucji. Uzyskany profil redystrybucji w stopie Fe-4.34Ni został porównany z profilem uzyskanym dla dubletonowej struktury stopu Al-3.5Li, w której nie obserwuje się reakcji perytektycznej. W tym ostatnim, zgodnie z przewidywaniami, ujawniono wydzielenia eutektyczne stosując technikę SEM. Sformułowano równania, pozwalające wyznaczyć krzywą teoretyczną redystrybucji i zestawić ją z odpowiednimi punktami pomiarowymi uzyskanymi z zamrożonej struktury stopu Fe-4.34Ni. Równania są analityczne i opisują przebieg reakcji perytektycznej; opracowane zostały z wykorzystaniem znajomości metastabilnej linii *solidus* na diagramie fazowym Fe-Ni. Ponadto, techniką dyfrakcji elektronów wstecznie rozproszonych (EBSD) określono orientację dubletonów stopu Al-3.5Li, krystalizujących i zamrożonych podczas testu mikrograwitacyjnego.

1. Introduction

Solute redistribution and the amount of precipitates are the factors limiting the properties of alloys produced by the different foundry technologies. Therefore, the prediction of inhomogeneity are valuable information for technologists.

The Fe-4.34Ni and Al-3.5Li alloys solidification was stopped during oriented cellular growth and a doublet shaped solid/liquid interface was frozen. The freezing of the oriented structure allowed the solute redistribution to be measured in respect of the geometry of cellular structure. The Li-solute redistribution was evaluated within a given doublet using neutron radiography with a cold neutron beam and neutron induced auto-radiography, [1]. The Ni-solute redistribution was measured by the use of EDXS technique. The initial concentration of the Ni-solute was chosen in order to ensure precipitation of the primary

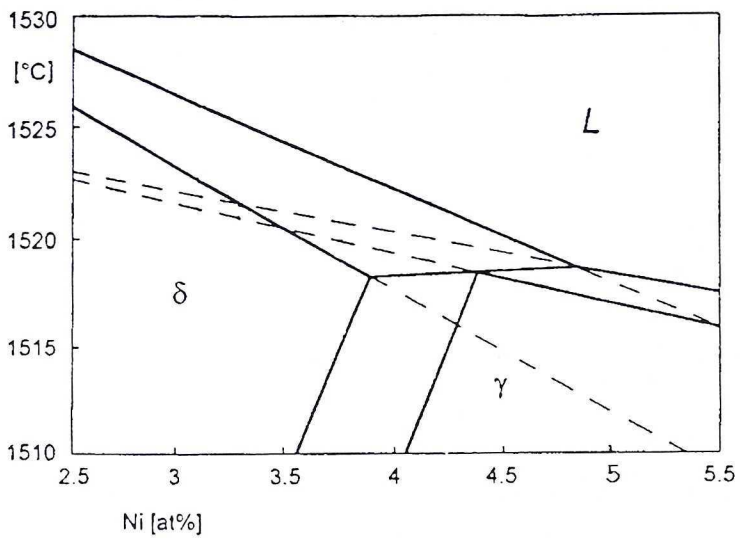

Fig. 1 Fe-Ni system with *metastable solidus* and *metastable liquidus* applied to simulation of the Ni-solute redistribution within the cellular morphology of the Fe-4.34Ni alloy, [3]

δ phase and $\delta + L = \gamma$ peritectic reaction as well, Fig. 1. In the case of the Al-Li system the only reaction was the eutectic one. The well known theory of solute redistribution, [2], is

only able to reproduce a profile of solute redistribution for the solidification of an alloy with eutectic reaction. Thus, the theory of solute redistribution worked out for simple eutectic system, [2], is to be developed in order to reproduce a solute redistribution for the system in which peritectic reaction can occur as it happens in the studied Fe-Ni system.

The EDXS technique was used in order to measure the solute redistribution and the amonut of precipitates. However, the effect crystal orientation on solute redistribution can be qualitatively evaluated by use of the EBSD technique.

D_S – diffusion coefficient in the solid, [m^2/s],
$\bar{H}$ – total height of cell used in standardization, [m],
k_1 - equilibrium partition ratio for the first range of solidification: $N_0 \rightarrow N_1$, as can be seen in Fig. 1 for the δ - phase growth, [mole fr./mole fr.],
k_2 - equilibrium partition ratio for the second range of solidification: $N_1 \rightarrow N_2$, as can be seen in Fig. 1 for the γ - phase growth, [mole fr./mole fr.],
$\bar{L}$ - half the cell spacing used in standardization, (Fig. 3), [m],
$\bar{L}_0$ - position of the s/l interface used in standardization, [m],
$\bar{L}_{0i}$ - co-ordinates of measurement points along the envelope of a standard cell, [m],
N_0 - nominal concentration of solute in a given alloy, [mole fr.],
N_1 - solute content in the liquid taking part in first peritectic reaction, [mole fr.],
N_2 - solute content in the liquid taking part in second peritectic reaction, [mole fr.],
N_{exp} - solute content determined experimentally, [mole fr.],
N_1^B - solute redistribution for the first range of solidification: $N_0 \rightarrow N_1$, [mole fr.],
N_1^S - solute content at the s/l interfaces existing during crystal growth for the first range of solidification: $N_0 \rightarrow N_1$, [mole fr.],
p_2 - partition ratio of the solute between left boundary of the γ phase (in the phase diagram, Fig. 1) and *liquidus* line, [mole fr./mole fr.],
t_f - local solidification time, [s],
v - crystal growth rate in the *Bridgman's* system, [m/s],
v_p - rate of cell thickening, [m/s],
x - amount of growing cell, normalised,
x_0 - amount of crystal frozen at a given stage of growth related to the standard cell, normalised,
x_0^i - amount of crystal related to the $\bar{L}_{0i}$ co-ordinates of measurement points, normalised,
x_i - amount of crystal related to a given measurement points λ_i, for a certain height of cell, as shown in Fig. 3, normalised,
X^0 - amount of crystal frozen at a given stage of growth, normalised,
X_1^0 - amount of crystal frozen at a given stage of growth within first range of solidification, normalised,
X_K - total amount of crystal at the end of growth, normalised,
x_1^m - amount of primary crystal δ which does not take part in solid/solid transformation, for the first range of solidification, normalised,

x_I^{min} - amount of primary crystal δ which does not take part in peritectic reaction for the first range of solidification, normalised,

x_I^{max} - amount of primary crystal δ and peritectic phase (sum) for the first range of solidification, normalised,

x_1^{tr} - amount of primary phase which remains after solid/solid transformation, for the first range of solidification, normalised,

Y - half cell spacing (Fig. 15) or measurement distance (Fig. 5-11), [m],

Y_0 - position of solid/liquid interface on the λ-axis, (Fig. 15), [m],

Y_K - position of solid/liquid interface on the λ-axis at the completion of crystal growth; boundary: crystal/precipitates, [m],

α_1^D - parameter of back-diffusion for the formation of primary crystal within the first range of solidification,

α_1^P - parameter of back-diffusion for the peritectic reaction within the first range of solidification,

β_1 - coefficient of redistribution for the first range of solidification,

λ - horizontal axis perpendicular to cell axis of symmetry, [m],

λ_i - co-ordinates of measurement points for standard cell, (Fig. 3), [m].

2. EDXS measurements of Ni-solute redistribution and EBSD analysis of Al-3.5Li doublet orientation

A frozen cell of the Fe-4.34Ni alloy has been selected for solute redistribution measurements, Fig. 2, according to one of four types of measurement line localization

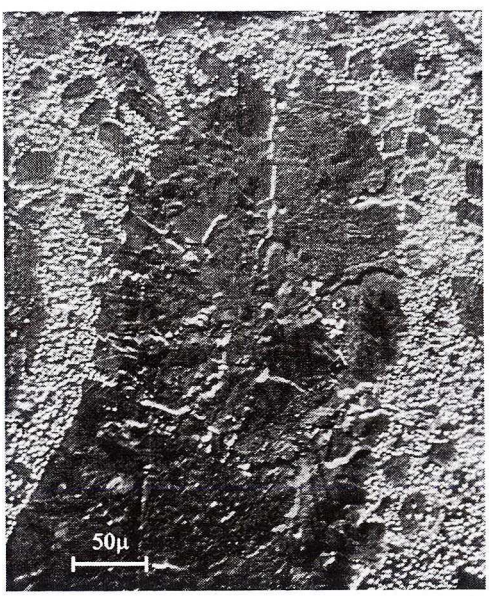

Fig. 2 Doublet shaped interface of the ferrite phase within the Fe-4.34Ni alloy

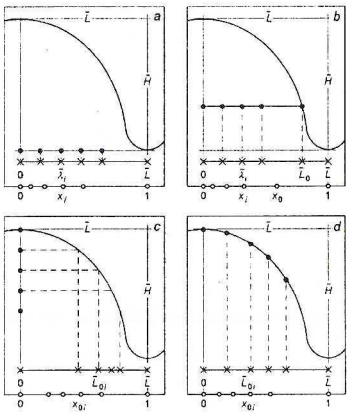

Fig. 3 Four types of the EDXS – analysis predicted for directional cellular morphology (2D solidification); scheme worked out for half a cell; a/ at the bottom of a cell, b/ at certain height of a cell, c/ along the axis of symmetry of a cell, d/ along the envelop of a cell

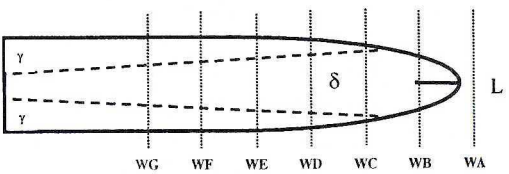

Fig. 4 Localization of *linescans* within schematically drawn cell in which $\delta + L = \gamma$ peritectic reaction is marked

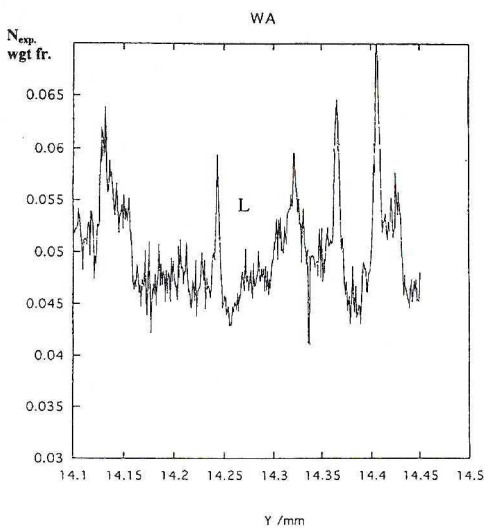

Fig. 5 Ni-solute redistribution across the liquid surrounding the selected doublet of the Fe-4.34Ni alloy, according to WA-measurement line shown in Fig. 4

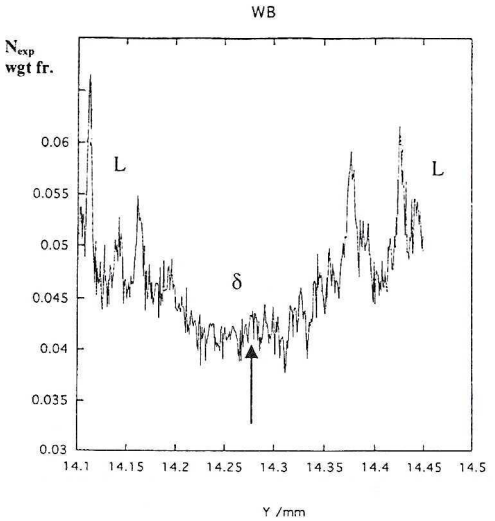

Fig. 6 Ni-solute redistribution across the selected doublet tip of the Fe-4.34Ni alloy, according to WB-measurement line shown in Fig. 4; arrow indicates the increase of the solute content related to the tip splitting

available due to delivered model, [2], Fig. 3. Thus, the b⁄ method (Fig. 3) has been applied for the investigation of the Ni solute redistribution within selected cell. Measurements have been performed at different heights of the cell as it is shown in Fig. 4. The results of Ni-solute redistribution measurement illustrate not only the intensity of segregation but also a development of the δ – phase formation from the liquid, Figs. 5–6, and the $\delta + L = \gamma$ peritectic reaction, Figs. 7–11, as well.

The analysis of cell tip geometry, Fig. 4, revealed that the cell tip is a doublet shaped solid/liquid interface. A similar doublet shaped solid/liquid interface was observed in the case of oriented growth of the Al-3.5Li alloy during microgravity test, Fig. 12a, [1]. Solidification of the Al-3.5Li alloy should be usually accompanied by eutectic precipitation, Fig. 12. It has been confirmed by use of SEM/EBSD observations, Fig. 13.

It is well known that the oriented growth leads to the formation of cell with privilege orientation. However, in the case of cell with doublet shaped solid/liquid interface, the orientation of each half split cell seems to be not the same as an orientation of the single crystal substrate from which doublets begin to form. It is evident that the tip splitting can play an essential role in doublets growth.

Electron backscatter diffraction applied to Al-3.5Li alloy cell proved that each doublet a has privilege plane to growth mainly the (126) plane, Fig. 14a. It should be emphasised that the [126] direction is only slightly deviated from the [001] direction of growth characteristic for the single crystal substrate.

It seems that such a rotation from (001) to (126) resulting from the formation of doublets asymmetry is not possible. Thus, it was concluded that the (001) orientation remains practically unchanged, Fig. 14b, however a divergence between axis of symmetry of doublet and directions of both parts of doubleton is formed. It seems to be justified because

both analysed orientations are similar. The above deviation was measured by use of EBSD method, Fig. 14c and its value was estimated as 16°75′. The EBSD measurements were complicated by the fact that doublets are not growing vertically, Fig. 4, Fig. 12a and crystal coordinates system was not precisely established. Forwardscatter electron image, Fig 13a, presents the topography of the Al-3.5Li alloy. It is clearly seen that protruding cells are surrounded by areas filled with fine grain eutectic. Such areas do not produce analysable diffraction patterns due to resolution limits of the EBSD technique. Crystal orientation map acquired from the scanned area is presented in Fig. 13b. It was found that the ideal orientation can be described by three *Euler* angles: $\varphi_1 = 290°$, $\Phi = 19°$ and $\varphi_2 = 30°$ which roughly responds to (126) orientation in *Miller* indices. The map was displayed in a texture component mode which allows to highlight data of particular orientation using the grey scale which reflects how close to ideal orientation the data are. In this particular case the maximum deviation angle was about 2°. Points that deviate from the ideal orientation by more that this angle are not displayed i.e. these points appear as transparent. There is a strong deviation from ideal orientation of each analysed cell, as visible in Fig. 13b.

3. Segregation theory applied to Ni-redistribution experimental analysis

The simple redistribution model, [2] for alloys solidifying with eutectic precipitates shown in Fig. 13a, is developed to analyse solute redistribution modified by the $\sigma + L = \gamma$ peritectic reaction, Figs 7–11. However, a description of solute redistribution known in the model [2] can be applied to reproduce the segregation within a primary crystal δ of the Fe-4.34Ni alloy. The solute redistribution written for one step solidification is given as follows, [2]:

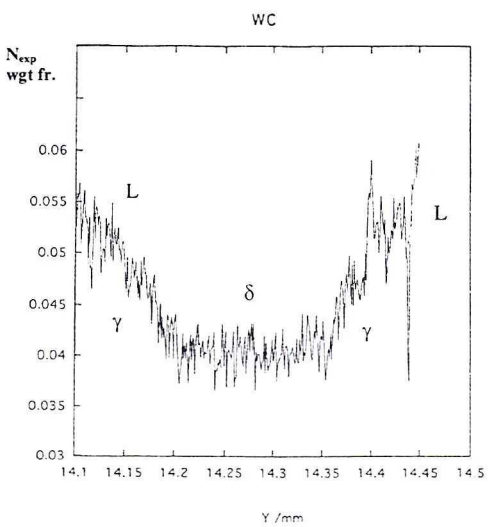

Fig. 7. Ni-solute redistribution across the selected doublet of the Fe-4.34Ni alloy, according to WC-measurement line shown in Fig. 4; parts of the measurement curve are related to the $\delta + L = \gamma$ peritectic reaction

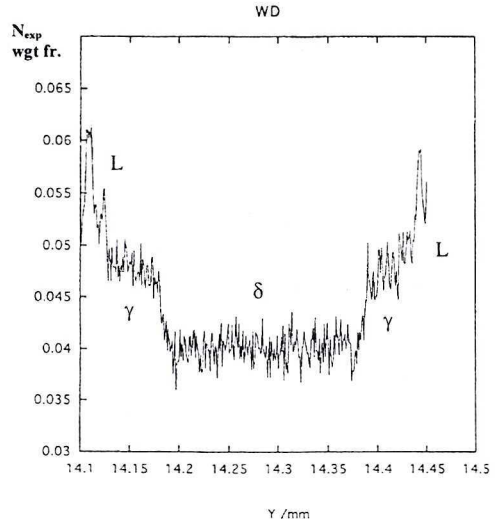

Fig. 8. Ni-solute redistribution across the selected doublet of the Fe-4.34Ni alloy, according to WD-measurement line shown in Fig. 4; parts of the measurement curve are related to the $\delta + L = \gamma$ peritectic reaction

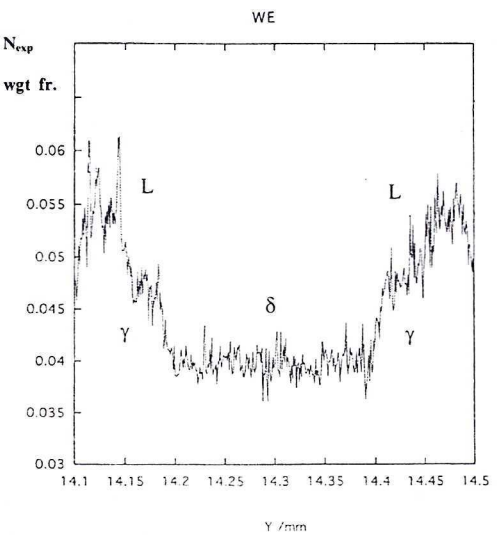

Fig. 9. Ni-solute redistribution across the selected doublet of the Fe-4.34Ni alloy, according to WE-measurement line shown in Fig. 4; parts of the measurement curve are related to the $\delta + L = \gamma$ peritectic reaction

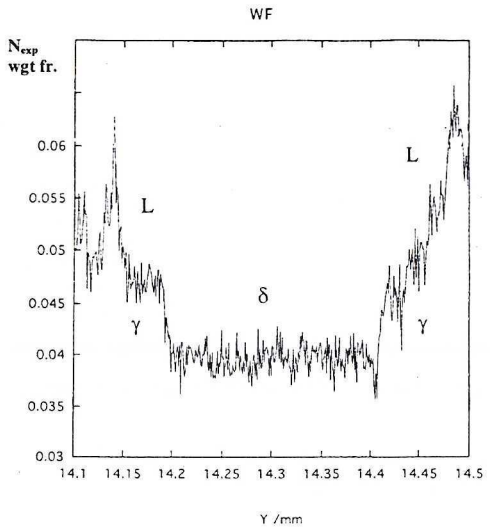

Fig. 10. Ni-solute redistribution across the selected doublet of the Fe-4.34Ni alloy, according to WF-measurement line shown in Fig. 4; parts of the measurement curve are related to the $\delta + L = \gamma$ peritectic reaction

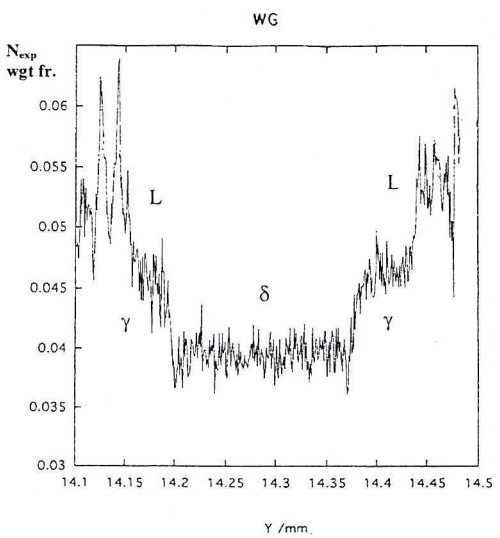

Fig. 11. Ni-solute redistribution across the selected doublet of the Fe-4.34Ni alloy, according to WG-measurement line shown in Fig. 4; parts of the measurement curve are related to the $\delta + L = \gamma$ peritectic reaction

$$N_1^B(x;\, X_1^0,\, \alpha_1^D) = \left[1 + \frac{\beta_1(x;\, X_1^0,\, \alpha_1^D)}{k_1}\right] N_1^S(x;\, \alpha_1^D) \qquad x \in [0, X_1^0], \tag{1}$$

where

$$N_1^S(x;\ \alpha_1^D) = k_1 N_0 (1 + \alpha_1^D k_1 x - x)^{(k_1 - 1)/(1 - \alpha_1^D k_1)} \tag{2}$$

Equation (2) describes the solute microsegregation at the solid/liquid interface drawn schematically in Fig. 15. Equations (1) and (2) are sufficient to describe the formation of solute redistribution and the amount of precipitate as illustrated experimentally in Fig. 13. However, the $\delta + L = \gamma$ peritectic reaction occurs during crystal growth of Fe-4.34Ni alloy, Figs 7–11. The amount of peritectic phase, γ, is increasing during experiment, which has been plotted schematically in Fig. 4. The amount of peritectic phase is denoted as the difference $x_1^{\max} - x_1^{\min}$. The $x_1^{\max}$ boundary can be calculated in following way:

$$x_1^{\max}(\alpha_1^D, \alpha_1^P) - x_1(\alpha_1^D) = A_1(x_1(\alpha_1^P, k_2) - x_1(\alpha_1^P, k_1)) \qquad 0 \le A_1 \le 1, \tag{3}$$

where

$A_1 = 0$ for the non-equilibrium solidification (Scheil's type process),

$A_1 = 1$ for equilibrium solidification (lever rule).

The A_1 – parameter is responsible for intensity of diffusion during peritectic reaction and is related to the α_1^P – parameter. The parameter $A_1 = 0$, when $\alpha_1^P = 0$ and $A_1 = 1$, when $\alpha_1^P = 1$. Thus, the maximum amount of peritectic phase is produced during equilibrium solidification and minimum amount of peritectic phase during non-equilibrium solidification, respectively. The amount of peritectic phase depends on the value of back-diffusion parameter α_1^P and it is evident that for the Scheil's mode of solidification, for which $\alpha_1^P = 0$, there is no peritectic phase; $x_1^{\max} - x_1^{\min} = 0$, that is $x_1^{\min} = x_1 = x_1^{\max}$. The concept of *metastable solidus*, Fig., 1 was employed in formulation of equation (3).

Then, the difference $x_1 - x_1^{\min}$ was calculated, taking into account the mass balance for the peritectic reaction:

$$\int_0^{x_1^{\min}} \left[N_1^B(x + x_1 - x_1^{\min},\ \alpha_1^D) - N_1^B(x,\ \alpha_1^D)\right] dx + \int_{x_1^{\min}}^{x_1} \left[k_2 N_1 - N_1^B(x,\ \alpha_1^D)\right] dx =$$
$$(N_1 - k_2 N_1)\left[x_1^{\max}(X_1^0,\ \alpha_1^D,\ \alpha_1^P) - x_1(\alpha_1^D)\right]. \tag{4}$$

The above equations are used in reproduction of the Ni-solute segregation measured previously at different heights of cell shown in Fig. 2, according to the scheme plotted in Fig. 4. An analysis of phase diagram, Fig. 1 suggests that solidification occurring within the second range (after completion of peritectic reaction is accompanied by the δ/γ transformation). Thus, it was concluded that the δ – phase, revealed experimentally, Figs. 5–11, results from both peritectic reaction and solid/solid transformation. These phenomena have already been discussed qualitatively, [4] but current equations give possibility to reproduce them in quantitative way, Fig. 16.

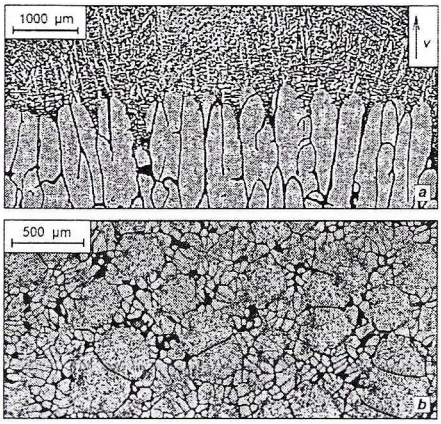

Fig. 12. Package morphology revealed within Al-3.5Li alloy frozen during microgravity test; a/ quenched interface revealing doublets, b/ 2D observation of cellular morphology

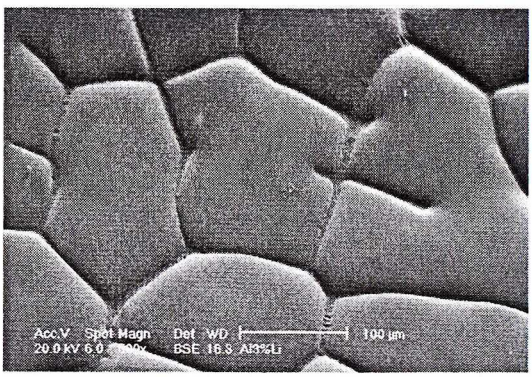

Fig. 13a. SEM micrograph of the Al-3.5Li alloy solidified directionally recorded by the use of forward scatter electrons collected by the set of solid state detectors attached to the CCD camera

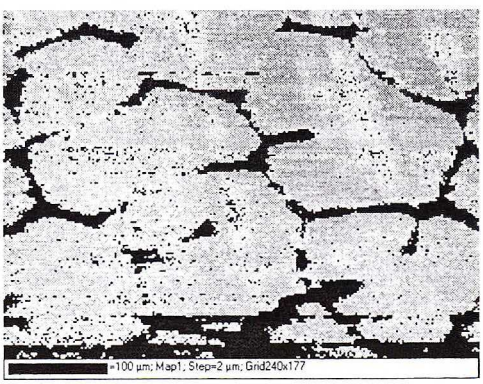

Fig. 13b. Crystal orientation map with the maximum deviation angle equal to 2°; the areas not producing analysable pattern are denoted in black colour

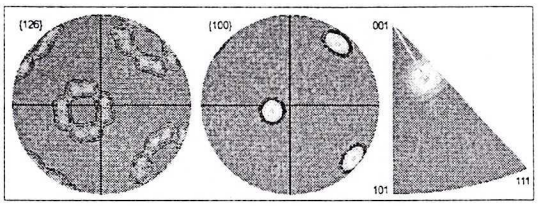

Fig. 14. Stereographic projection of: a/ {126}, b/ {100}, poles within oriented Al-3.5Li alloy, c/ inverse pole figure with the measurement of the angle between privilege growth direction and axis of a given doublet

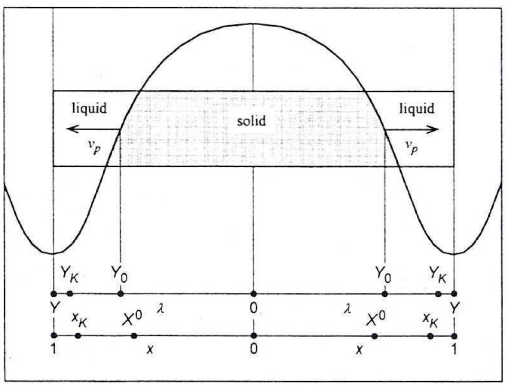

Fig. 15. 2D growth of a cell showing a cellular shape of frozen solid/liquid interface

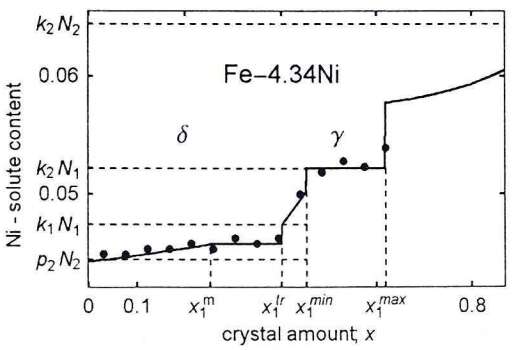

Fig. 16. Simulation of the Ni-solute segregation within Fe-4.34Ni alloy solidified with the presence of $\delta + L = \gamma$ peritectic reaction and δ/γ transformation; theoretical curve fitting the experimental Ni-solute redistribution shown for half a cell

The theoretical curve fits some measurement points, Fig. 16, where $0 \div x_1^{tr}$ denotes the primary phase δ; $x_1^{tr} \div x_1^{min}$ determines the γ phase resulting from the δ/γ transformation, $x_1^{min} \div x_1^{max}$ illustrates the γ phase resulting from the $\delta + L = \gamma$ peritectic reaction, $x_1^{max} <$ is related to the γ phase resulting from second range of solidification. Measurement points are taken from EDXS analysis run for half a cell, [4].

4. Discussion

The EDXS technique was applied to measure the Ni-solute segregation within directionally growing cells of Fe-4.34Ni alloy. The doublet tip splitting influences the solute segregation as it was the shown in Fig. 6. The interpretation of phase diagram, Fig. 1 from the point of view of the Ni-solute segregation Figs 5–11 allowed to identify both δ and γ phases within a given cell of doublet shaped solid/liquid interface, Fig. 2. The EBSD technique was applied to measure doublet privileged orientation and allowed to correlate it to the orientation of single crystal substrate from which analysed cell grows, Fig. 14.

Relevant equations were proposed to describe the formation of peritectic phase and the concept of *metastable solidus* line was used in order to establish equation (3). These equations used to reproduce of the Ni-solute segregation, Fig. 16. The $0 - x_1^m$ part of theoretical curve, Fig. 16, is a superposition of microsegregation curve, equation (2), and redistribution curve, equation (1), and finally corrected by diffusive shift curve resulting from the solute content increase necessary to ensure the peritectic reaction due to equilibrium phase diagram, Fig. 1. The $x_1^m - x_1^{tr}$ part of theoretical curve represents the Ni-solute segregation within the primary phase resulting from the cut of diffusive shift required by the formation of peritectic phase due to solid/solid transformation.

The theoretical curve fits well to measurement points which is promising for future reproductions of solute segregation in such a solidification process.

The presented equations are universal and can be used in reproduction of the solute segregation resulting from another solidification processes corresponding to the $1D$ or $3D$ crystal growth however, the reproduction requires, to recalculate properly the measurement distance into an amount of crystal due to a given geometry of crystal growth.

The influence of tip splitting onto the segregation cannot be yet interpreted by means of current equations.

Revealed rotation of orientation was measured within Al-3.5Li doublets for which the tip splitting had been more visible (EBSD analysis). It seems that expected double rotation is: [100] $\Rightarrow$ [126] $\Rightarrow$ [100]. The [100] orientation defines a single crystal substrate; [126] orientation determines both parts of the tip splitting, and again the [100] orientation describes the final product of honeycomb like morphology of a given solid solution.

EDXS measurements of solute segregation revealed only the existence of δ and γ phases within a given cell of the Fe-4.34Ni alloy. The theoretical reproduction of solute segregation has revealed that peritectic phase is to be related not only to the peritectic reaction but also to solid/solid transformation.

5. Conclusions

The theory developed to reproduce solute segregation reveals an solidification rate onto redistribution profile which is evident while the back-diffusion parameter α is analysed.

The theoretically reproduced profile seems to be in a good agreement with the measured profile of segregation. The fitting parameter is the back-diffusion parameter α. Its quantitative determination allows to estimate the value of diffusion coefficient into the solid, D_S.

The EBSD analysis show the rotation of crystal orientation. Such a rotation modifies leading to their asymmetry profiles of solute segregation.

REFERENCES

[1] G. Bayon, B. Drevet, R. Ilic, M. Humar, J. J. Rant, H. Nguyen-Thi, Proc. of the Fifth World Conf. on Neutron Radiography, eds C.O. Fischer, J. Stade, W. Bock, ed. Deutsche Gesellschaft fur Zerstorrungsfreie Prufung E.V., Berllin, 1996, 417.

[2] W. Wołczyński, Chapter 2 in: Modelling of Transport Phenomena in Crystal Growth, p. 19–59, ed. WIT Press, Southampton – Boston, 2000, eds. J. Szmyd & K. Suzuki.

[3] T. Okane, T. Umeda, Eutectic Growth of Unidirectionally Solidified Fe-Cr-Ni Alloy, ISIJ International, **38**, 454 (1998).

[4] J. Kloch, B. Billia, T. Okane, T. Umeda, W. Wołczyński, Experimental Verification of the Solute Redistribution in Cellular/Dendritic Solidification of the Al-3.5Li and Fe-4.34Ni Alloys, Materials Science Forum, **329/330**, 31 (2000).

REVIEWED BY: WOJCIECH KAPTURKIEWICZ

Received: 3 September 2003.